

Prediction of Half Metallicity along the Edge of Boron Nitride Zigzag Nanoribbons

Fawei Zheng¹, Gang Zhou¹, Zhirong Liu², Jian Wu¹,

Wenhui Duan^{1*}, Bing-Lin Gu¹, and S. B. Zhang³

¹*Center for Advanced Study and Department of Physics,
Tsinghua University, Beijing 100084, People's Republic of China*

²*College of Chemistry and Molecular Engineering,
Peking University, Beijing 100871, People's Republic of China*

³*Department of Physics, Applied Physics, and Astronomy,
Rensselaer Polytechnic Institute, Troy, NY 12180, USA*

(Dated: April 27, 2008)

Abstract

First-principles calculations reveal half metallicity in zigzag boron nitride (BN) nanoribbons (ZBNNRs). When the B edge, but not the N edge, of the ZBNNR is passivated, despite being a pure *sp*-electron system, the ribbon shows a giant spin splitting. The electrons at the Fermi level are 100% spin polarized with a half-metal gap of 0.38 eV and its conductivity is dominated by metallic single-spin states. The two states across at the Dirac point have different molecular origins, which signals a switch of carrier velocity. The ZBNNR should be a good potential candidate for widegap spintronics.

* Author to whom correspondence should be addressed. Email: dwh@phys.tsinghua.edu.cn

Half metallicity is at the forefront of spintronics study[1, 2, 3]. Half metallicity occurs when one of the electron spins shows insulating behavior while the other shows metallic behavior[4]. If one drives a current through such a half metallic system, the current will be 100% spin polarized. Obviously, 100% spin polarization could have many potential spin-related applications[1, 2]. For sometime now, it is understood that transition metal (TM)-containing systems such as ferromagnetic manganese perovskite will show half metallicity[5, 6]. The TM systems, however, may not be compatible with many of the matured technologies today that rely heavily on main group semiconductors. Heavy TM elements also often act as poison agents in biological systems. It is thus highly desirable to develop non-TM half metallic materials, especially if the half metallicity can be a byproduct of the existing electronic materials. To this end, it is quite encouraging to see that nanoscale zigzag graphene ribbons would show half metallicity under high in-plane homogeneous electric field[7], as graphene ribbons could be an ideal conducting material for future nanoelectronic applications[8]. However, intrinsic half metallicity without any external constraints is yet to be demonstrated and more desirable in many practical applications.

In searching for intrinsic half metallicity in main group semiconductors, we note that boron nitride (BN) nanoribbons may hold high promises. BN nanotubes (BNNTs), hexagonal *h*-BN, and nanoribbons (BNNRs) are the III-V analogues of the widely studied carbon nanotubes (CNTs), graphite, and graphene nanoribbons (GNRs). Different from their carbon counterparts, however, the BNNTs have a nearly constant band gap independent of radius and chirality[9]. The *h*-BN is, on the other hand, a wide gap semiconductor. Single layer *h*-BN has been successfully fabricated on the surfaces of metals [10]. The BNNRs are expected to be produced straightforwardly by using single layer *h*-BN as the starting material, but should have very different physical properties from those of *h*-BN due to quantum size and symmetry effects, and, as will be shown below, due to unexpected edge effects. More importantly, the properties of the BNNRs may also be qualitatively different from those of the GNRs, because of the relatively large ionicity and significantly larger band gap of the *h*-BN.

In this paper, we predict intrinsic half metallicity in BNNRs with zigzag edges (ZBNNRs) by first-principle calculations. The half-metal energy gap for ribbons with passivated boron edge is as high as 0.38 eV (about 15 times larger than $k_B T$ at $T = 300$ K). This does not require any applied external electric field, in contrast to the graphene ribbons. Our

analysis reveals that the half metallicity is originated from an interesting interplay between the nitrogen edge dangling bond state and the occupied nitrogen lonepair state, which is absent in the graphene systems. The crossing between the two states defines the Fermi level and hence the degree of half metallicity. The intrinsically different molecular orbital origins of the two states further suggest a switch of the carrier velocity across the Dirac point that is awaiting for experimental verification. The integration of half metallicity (at the ribbon edge) with widegap semiconductivity (of the ribbon backbone) also opens new application potentials whose full extent is yet to be explored.

The ZBNNRs we considered are schematically illustrated in Fig. 1, which are hexagonally bonded honeycomb ribbons consisting of B and N atoms with zigzag terminated edges under various passivations. In accordance with the previous convention [11], here the ZBNNRs are labeled by the number of parallel zigzag chains, which defines the width of the ribbon. The ZBNNR with n B-N chains is thus named as n -ZBNNR. For ZBNNRs, the outmost atoms at one edge (namely, the B-edge) are all B atoms, whereas the outmost atoms at the other edge (namely, the N-edge) are all N atoms. In terms of hydrogen passivation of the edges, the ZBNNRs are further divided into four subgroups [Fig. 1 (a)-(d)]: 1) both edges are passivated (ZBNNR-2H), 2) only the B-edge is passivated (ZBNNR-HB), 3) only the N-edge is passivated (ZBNNR-HN), and 4) no edge is passivated (pristine ZBNNR).

Our calculations were performed by using the density functional theory [12] within the local spin density approximation (LSDA). In particular, we used the Vanderbilt planewave ultrasoft pseudopotential [13], with a 450-eV cutoff energy, and the Ceperly-Alder exchange-correlation potential [14]. We adopted a supercell geometry for isolated BNNR sheet in which each two adjacent sheets are separated by at least 11 Å. For n -ZBNNRs, the supercell contains n [Fig. 1 (a) and (b)] or $2n$ [Fig. 1 (c) and (d)] BN atoms depending on whether dimerization of the edge atoms takes place or not. Integration over the one dimensional Brillouin zone (Γ - X) has been carried out by using 51 and 31 Monkhorst-Pack k -points, respectively [15], with the equivalent k -point scheme. Full optimization of the atomic structures including atomic positions and lattice parameters has been carried out until the residual forces on atoms are less than 0.01 eV/Å. We have also increased the size of the supercell to make sure that it does not produce any discernible difference on the results.

The electronic and magnetic properties of the BN nanoribbons depend critically on how the edges are passivated. Half metallicity is observed when and only when the boron edge

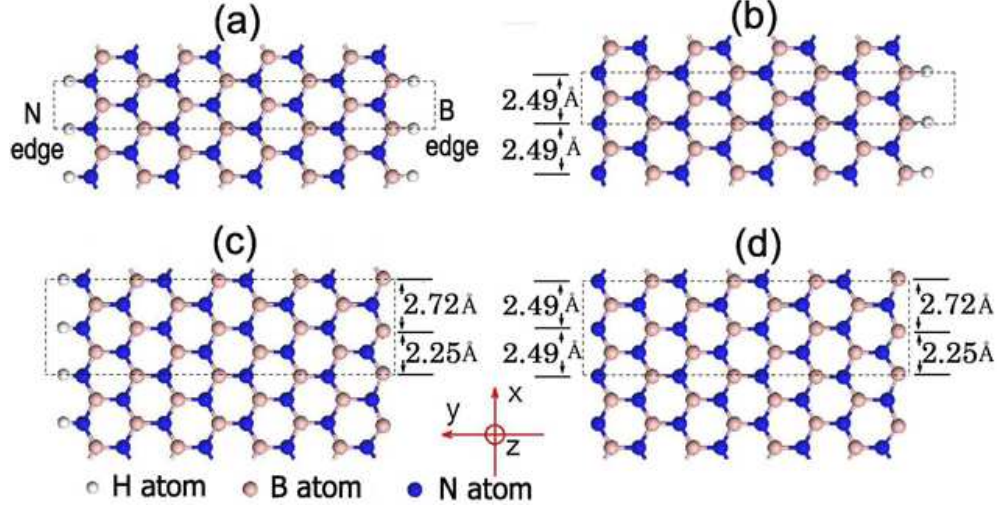


FIG. 1: (color online). Atomic geometries of the relaxed zigzag boron nitride nanoribbons (ZBNRs) with different edge treatments: (a) 8-ZBNR-2H, (b) 8-ZBNR-HB, (c) 8-ZBNR-HN, and (d) pristine 8-ZBNR, where the number 8 stands for the width of the ribbon, and the suffixes HB and HN stand for hydrogen termination of the boron and nitrogen edges, respectively. The ribbons are infinitely long along the x direction. The distances between two adjacent edge atoms are selectively shown in the figure. It should be noted that in (c) and (d), the edge B atoms are dimerized, resulting in two different edge B-B distances. The dashed rectangles denote the unit cell of the systems.

is passivated [Fig. 1(b)]. The band structures of the 8-ZBNR-HB are depicted in Fig. 2(a) and (b), which show marked differences in the spin states: the spin-down electrons are metallic with two bands (α and β) crossing each other at the Fermi level, while the spin-up ones are insulating due to the existence of a band gap as large as 4.5 eV. Thus, charge transport are totally dominated by the spin-down electrons [see the DOS in Fig. 2(c)], and current flow in such a system should be completely spin-polarized. The half-metal gap, defined as the difference between the Fermi level and topmost occupied spin-up band, is 0.38 eV. This value is comparable to that of half-metallic graphene nanoribbon under high electric field [7], and is large enough for room-temperature operation. In Fig. 2(d) and (e), we plot the partial charge density of the α and β bands (at the characteristic X point). One can see that the α and β bands are almost entirely localized on the N edge. All the ZBNRs-HB, regardless of their width, have a similar band structure.

In order to understand the band crossing responsible for the half-metallicity of ZBNRs-

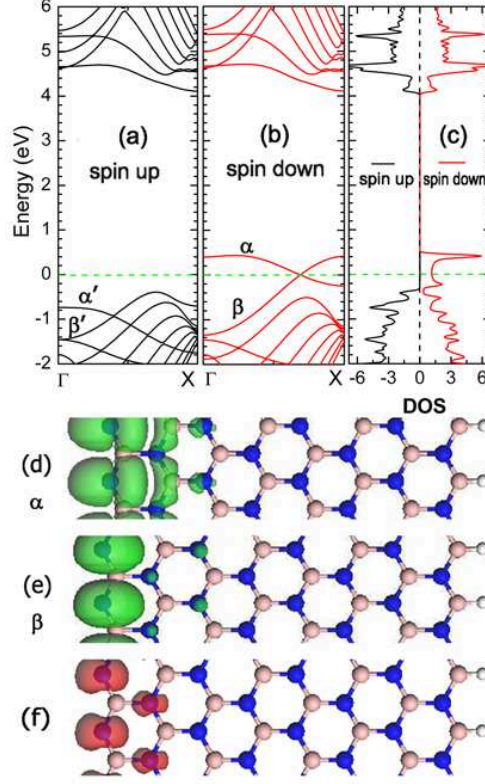


FIG. 2: (color online). Half metallic and ferromagnetic behaviors of 8-ZBNR-HB. (a) Spin-up and (b) spin-down energy bands, and (c) the total density of states (DOS). Here, the energy zero (i.e., the dot-dashed green line) is at the Fermi level. Γ and X denote the center and the boundary of the first Brillouin zone. (d) and (e) Partial charge density of the α and β band at the X point, respectively. The isosurface is $0.003 \text{ e}/\text{\AA}^3$. (f) Spatial distribution of the spin difference: red for spin-up and yellow for spin down. The isosurface is $0.03 \mu_B/\text{\AA}^3$. Due to the small amplitude of the spin-down states, they are not visible from the plot.

HB, we have studied how passivation at the N edge affects the electronic structure. With H passivation, the α band shifts down considerably to reside inside the valence band, while the β band is very much unchanged and is hence still above the top of the valence band. The projected density of states (PDOS) of the two bands show that the α band is predominantly composed of the nitrogen p_y and s atomic orbitals, while the β band is composed almost completely of the nitrogen p_z atomic orbitals. In other words, the α band is a dangling bond state at the N edge, and is hence strongly affected by the passivation. In contrast, the β band is the usual lonepair state of threefold coordinated nitrogen, and is by-in-large unaffected by the passivation. The wavefunctions of the α and β bands have different symmetries: being

symmetric and anti-symmetric, respectively, with respect to the basal plane of the BN sheet. These explain why the α and β bands in Fig. 2(b) cross each other without having to create a band gap. If we bend the BN sheet or apply an electric field along the z -direction to break such a mirror symmetry, however, the α band will mix with the β band, but the total energy of the system also increases. For example, when the 8-ZBNNR-HB ribbon is bent to 90° around the x axis, the total energy increases by 0.2 eV per unit cell. We have checked the spin-up α' and β' bands below the Fermi level to find that they too have the same atomic characters of the spin-down α and β bands.

An essential factor underlying the observed half metallicity is the splitting of the spin states. In fact, Fig. 2(f) shows that the ground state of the ZBNNRs-HB is *ferromagnetic* with a magnetic moment of $1 \mu_B$ per edge N atom. The calculated magnetic interaction is quite large: for instance, the ferromagnetic phase is 0.10 eV per edge N atom more stable than the anti-ferromagnetic phase, and is also 0.17 eV per edge N atom more stable than the nonmagnetic phase. Importantly, these energy differences are independent of the ribbon width n when $n \geq 5$. A relatively large distance (2.49 Å) between any two adjacent edge N atoms implies that no edge reconstruction has taken place, and there is thus one dangling bond per edge N atom. From such an analysis, we conclude that magnetism is a result of the exchange interaction between dangling bond electrons. Similar magnetic ordering in a dangling bond network was also observed on partially hydrogenated Si(111) surfaces [16].

An obvious concern with the above discussion is the LDA band gap error, which in principle could change the qualitative band structure near the Fermi level in Fig. 2(b). To address such a concern, we have calculated 3-ZBNNR-HB with the GW approximation[17] by using the ABINIT code [18]. The results show that the system remains to be half-metallic with band crossing at the Fermi level, despite significant quasiparticle corrections to the LDA band structure, particularly in the conduction bands[19].

In recent years, graphene has emerged as a new model system in materials science and condensed matter physics due to its novel physical properties [20]. For example, graphene is the first material where electron transport was found to be governed by the relativistic Dirac equation: namely, energy dispersion $E(k)$ with respect to wavevector k is linear, so that charge carriers mimic the relativistic quasiparticles with zero rest mass (the so-called Dirac fermions) and travel with an effective “speed of the light”, $v = E/k$, on the order of $\sim 10^6$ m/s [21]. Thus, it is important that our ZBNNRs-HB also exhibits such an unusual

massless Dirac-fermion behavior. Due to the intrinsic difference between the α and β bands, however, the two bands at the crossing point will have different slopes, corresponding to different v 's. This, combined with the unique one-dimensional characteristics of the edge states, suggests new physics that cannot exist in the graphene systems with “symmetric” energy dispersion.

When the N-edge, and only the N-edge, is passivated, the system, ZBNNRs-HN, behaves qualitatively different. Figure 1c shows that here a dimerization of the boron atoms at the bare B-edge takes place spontaneously to lower the energy by 0.27 eV/dimer. The system is no longer spin-polarized, but semiconducting with a gap of 1.44 eV as shown in Fig. 3(a). The B-B dimer has an equilibrium bondlength of 2.25 Å, which leaves the B-B distance between two adjacent dimers to be 2.72 Å. The calculated partial charge densities of the highest occupied γ band and the lowest unoccupied δ band in Fig. 3(b) reveal that both states are localized at the bare B edge. Bands γ and δ exhibit the typical characteristics of a bonding and anti-bonding orbital, respectively. This suggests that the unpaired dangling bond states of the boron atoms have rehybridized considerably. Note that edge boron dimerization is a common phenomenon, which has been observed in the simulation of the BNNT growth [22] and for the B-rich mouth of open zigzag BNNTs [23].

Dimerization is crucial for the disappearance of half metallicity. If we prohibit the dimerization by artificially using a unit cell that contains only n B (N) atoms as those in Fig. 1(a) and (b), the half metallicity and ferromagnetic behaviors will reappear. For pristine ZBNNRs with no edge passivation, edge B atoms will dimerize but edge N atoms will not, as shown in Fig. 1(d). This system is also half metallic but with a negligible half-metal energy gap of only 0.08 eV (see Supplementary Material for details of the band structure[19]). When both edges are passivated, on the other hand, the system, e.g., ZBNNR-2H in Fig. 1(a), is nonspin-polarized and has a wide band gap. Our results here qualitatively agree with the earlier work by Nakamura *et al.* [24].

To experimentally realize half metallicity in ZBNNRs, two key issues must be addressed: (1) The choice of the substrate. Chemical activity of the available substrates is often diverse, which should be utilized to advance our course. For example, if one wishes to minimize the influence of the substrate, an inert substrate should be used as was the case in fabricating single layer *h*-BN[10]. (2) Selective passivation. In the current study, hydrogen has been used as the passivant for its simplicity. The drawback of using H is clear as the selectivity

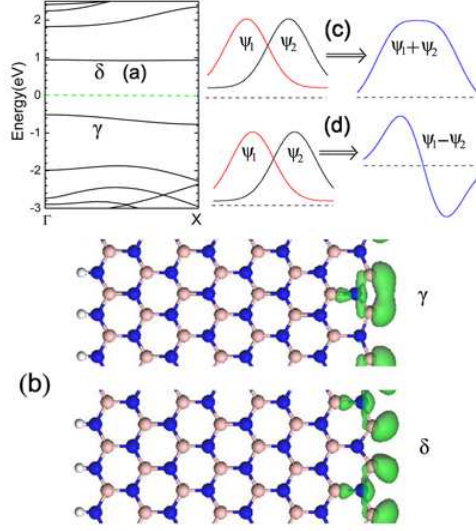


FIG. 3: (color online). Electronic properties and edge dimerization of 8-ZBNR-HN. (a) Energy band structure. The γ and δ bands are the highest valence and the lowest conductance bands, respectively. Energy zero is at the nominal Fermi level position (i.e., the green dashdotted line). (b) Partial charge densities of the γ and δ bands at the X point. The isosurface is $0.03 e/\text{\AA}^3$. (c) and (d) Schematic drawing of the formation of bonding and anti-bonding orbitals from two adjacent atomic states.

can be rather poor. To optimize the selectivity, one might make good use of the chemical difference between B and N. For example, a more electronegative passivant such as F may be superior for boron passivation to yield the desired half metallicity but may not work at all for nitrogen passivation.

In summary, first-principles study reveals half metallicity in ZBNRs. Specifically, boron edge passivated nanoribbons, ZBNRs-HBs, is a half-metal with a half-metal gap of 0.38 eV. Non-d ferromagnetism and completely spin-polarized current transport may thus be possible. Nitrogen edge passivated nanoribbons, ZBNR-HN are, on the other hand, nonmagnetic and semiconducting. These unique properties, especially the half-metallicity, make the BN nanoribbons attractive candidate for nanoscale widegap spintronics such as spin-injection electrode, nano memory elements, and nano transistors.

SBZ thanks Damien West for valuable discussions. This work was supported by the National Natural Science Foundation of China (Grant Nos. 10325415, 10674077, and 10774084) and the Ministry of Science and Technology of China (Grant Nos. 2006CB605105 and

2006CB0L0601). SBZ was supported by the US DOE/BES and EERE under the contract No. DE-AC36-99GO10337.

- [1] G. A. Prinz, Science **282**, 1660 (1998).
- [2] S. A. Wolf, D. D. Awschalom, R. A. Buhrman, J. M. Daughton, S. von Molnar, M. L. Roukes, A. Y. Chtchelkanova, and D. M. Treger, Science **294**, 1488 (2001).
- [3] M. Ziese, Rep. Prog. Phys. **65**, 143 (2002).
- [4] R. A. de Groot, F. M. Mueller, P. G. van Engen, and K. H. J. Buschow, Phys. Rev. Lett. **50**, 2024 (1983).
- [5] J. -H. Park, E. Vescovo, H. -J. Kim, C. Kwon, R. Ramesh and T. Venkatesan, Nature **392**, 794 (1998).
- [6] C. M. Fang, G. A. de Wijs and R. A. de Groot, J. Appl. Phys. **91**, 8340 (2002).
- [7] Y. -W. Son, M. L. Cohen and S. G. Louie, Nature **444**, 347 (2006).
- [8] K. Wakabayashi, Y. Takane, M. Sigrist, Phys. Rev. Lett. **99**, 036601 (2007).
- [9] X. Blase, A. Rubio, S. G. Louie, and M. L. Cohen, Europhys. Lett. **28**, 355 (1994); E. Hernández, C. Goze, P. Bernier, and A. Rubio, Phys. Rev. Lett. **80**, 4502 (1998); Y. Chen, J. Zou, S. J. Campbell, and G. Le Caer, Appl. Phys. Lett. **84**, 2430 (2004); A. P. Suryavanshi, M. Yu, J. Wen, C. Tang, and Y. Bando, Appl. Phys. Lett. **84**, 2527 (2004).
- [10] A. Nagashima, N. Tejima, Y. Gamou, T. Kawai, and C. Oshima, Phys. Rev. Lett. **75**, 3918 (1995); M. Corso, T. Greber, and J. Osterwalder, Surf. Sci. **577**, 78 (2005).
- [11] K. Nakada, M. Fujita, G. Dresselhaus, and M. S. Dresselhaus, Phys. Rev. B **54**, 17954 (1996); K. Wakabayashi, M. Fujita, H. Ajiki, and M. Sigrist, Phys. Rev. B **59**, 8271 (1999).
- [12] Calculations were performed using the Vienna *Ab initio* Simulation Package (VASP). See, G. Kresse and J. Furthmüller, Comput. Mater. Sci. **6**, 15 (1996) and references therein.
- [13] D. Vanderbilt, Phys. Rev. B **41**, R7892 (1990).
- [14] D. M. Ceperley and B. J. Alder, Phys. Rev. Lett. **45**, 566 (1980).
- [15] H. J. Monkhorst and J. D. Pack, Phys. Rev. B **13**, 5188 (1976).
- [16] S. Okada, K. Shiraishi, and A. Oshiyama, Phys. Rev. Lett. **90**, 026803 (2003).
- [17] M.S. Hybertsen and S.G. Louie, Phys. Rev. B **34**, 5390 (1986); S. B. Zhang, et al., Phys. Rev. B **40**, 3162 (1989).

- [18] The ABINIT code was developed by the Université Catholique de Louvain, Corning Incorporated, and other contributors (URL:<http://www.abinit.org>).
- [19] EPAPS Document No. []. A direct link to this document may be found in the online article HTML reference section. For more information, see <http://www.aip.org/pubservs/epaps.html>.
- [20] A. K. Geim and K. S. Novoselov, *Nature Mater.* **6**, 183 (2007).
- [21] K. S. Novoselov, A. K. Geim, S. V. Morozov, D. Jiang, M. I. Katsnelson, I. V. Grigorieva, and S. V. Dubonos, *Nature* **438**, 197 (2005).
- [22] X. Blase, A. De Vita, J.-C. Charlier, and R. Car, *Phys. Rev. Lett.* **80**, 1666 (1998).
- [23] S. G. Hao, G. Zhou, W. H. Duan, J. Wu, and B. L. Gu, *J. Am. Chem. Soc.* **128**, 8453 (2006).
- [24] J. Nakamura, T. Nitta, and A. Natori, *Phys. Rev. B* **72**, 205429 (2005).